

Highly efficient Raman distributed feedback fibre lasers

Jindan Shi,* Shaif-ul Alam, and Morten Ibsen

Optoelectronics Research Centre, University of Southampton, Highfield, Southampton, SO17 1BJ, UK

*jxs@orc.soton.ac.uk

Abstract: We demonstrate highly efficient Raman distributed feedback (DFB) fibre lasers for the first time with up to 1.6W of continuous wave (CW) output power. The DFB Bragg gratings are written directly into two types of commercially available passive germano-silica fibres. Two lasers of 30cm length are pumped with up to 15W of CW power at 1068nm. The threshold power is ~2W for a Raman-DFB (R-DFB) laser written in standard low-NA fibre, and only ~1W for a laser written in a high-NA fibre, both of which oscillate in a narrow linewidth of <0.01nm at ~1117nm and ~1109nm, respectively. The slope efficiencies are ~74% and ~93% with respect to absorbed pump power in the low-NA fibre and high-NA fibre respectively. Such high conversion efficiency suggests that very little energy is lost in the form of heat through inefficient energy transfer. Our results are supported by numerical simulations, and furthermore open up for the possibility of having narrow linewidth all-fibre laser sources in wavelength bands not traditionally covered by rare-earth doped silica fibres. Simulations also imply that this technology has the potential to produce even shorter R-DFB laser devices at the centimetre-level and with mW-level thresholds, if Bragg gratings formed in fibre materials with higher intrinsic Raman gain coefficient than silica are used. These materials include for example tellurite or chalcogenide glasses. Using glasses like these would also open up the possibility of having narrow linewidth fibre sources with DFB laser oscillating much further into the IR than what currently is possible with rare-earth doped silica glasses.

©2012 Optical Society of America

OCIS codes: (060.3735) Fiber Bragg gratings; (140.3490) Lasers, distributed-feedback; (140.3550) Lasers, Raman; (140.3510) Lasers, fiber.

References and links

1. J. T. Kringlebotn, J.-L. Archambault, L. Reekie, and D. N. Payne, "Er³⁺:Yb³⁺-codoped fiber distributed-feedback laser," *Opt. Lett.* **19**(24), 2101–2103 (1994).
2. A. Asseh, H. Storøy, J. T. Kringlebotn, W. Margulis, B. Sahlgrén, S. Sandgren, R. Stubbe, and G. Edwall, "10cm Yb³⁺ DFB fibre laser with permanent phase shifted grating," *Electron. Lett.* **31**(12), 969–970 (1995).
3. M. Ibsen, E. Rønnekleiv, G. J. Cowle, M. O. Berendt, O. Hadeler, M. N. Zervas, and R. I. Laming, "Robust high power (>20 mW) all-fibre DFB lasers with unidirectional and truly single polarisation outputs," in *Proceedings of CLEO '99*, paper CWE4 (1999).
4. K. O. Hill, B. S. Kawasaki, and D. C. Johnson, "Low-threshold cw Raman laser," *Appl. Phys. Lett.* **29**(3), 181–183 (1976).
5. P. Persephonis, S. V. Chernikov, and J. R. Taylor, "Cascaded CW fibre Raman laser source 1.6–1.9 μm ," *Electron. Lett.* **32**(16), 1486–1487 (1996).
6. Y. Feng, L. R. Taylor, and D. B. Calia, "150 W highly-efficient Raman fiber laser," *Opt. Express* **17**(26), 23678–23683 (2009).
7. S. K. Turitsyn, S. A. Babin, A. E. El-Taher, P. Harper, D. V. Churkin, S. I. Kablukov, J. D. Ania-Castanon, V. Karalekas, and E. V. Podivilov, "Random distributed feedback fibre laser," *Nat. Photonics* **4**(4), 231–235 (2010).
8. R. Engelbrecht, A. Siekiera, R. Bauer, R. Neumann, and B. Schmauss, "Characterization of Short PM Raman Fiber Lasers with a Small Spectral Bandwidth," in *Proceedings of OFC/NFOEC '11*, paper OMQ2 (2011).
9. V. E. Perlin and H. G. Winful, "Distributed feedback fiber Raman laser," *IEEE J. Quantum Electron.* **37**(1), 38–47 (2001).
10. H. Kogelnik and C. V. Shank, "Coupled wave theory of distributed feedback lasers," *J. Appl. Phys.* **43**(5), 2327–2335 (1972).

11. Y. Hu and N. G. R. Broderick, "Improved design of a DFB Raman fibre laser," *Opt. Commun.* **282**(16), 3356–3359 (2009).
12. J. Shi and M. Ibsen, "Effects of Phase and Amplitude Noise on π Phase-Shifted DFB Raman Fibre Lasers," in Proceedings of *BGPP'10*, paper JThA30 (2010).
13. P. S. Westbrook, K. S. Abedin, J. W. Nicholson, T. Kremp, and J. Porque, "Demonstration of a Raman fiber distributed feedback laser," in Proceedings of *CLEO'11*, PDPA11 (2011).
14. P. S. Westbrook, K. S. Abedin, J. W. Nicholson, T. Kremp, and J. Porque, "Raman fiber distributed feedback lasers," *Opt. Lett.* **36**(15), 2895–2897 (2011).
15. J. Shi, S.-u. Alam, and M. Ibsen, "High power, low threshold, Raman DFB fiber lasers," in Proceedings of IQEC/CLEO Pacific Rim Sydney, postdeadline paper (2011).
16. M. Ibsen, M. K. Durkin, M. J. Cole, and R. I. Lamming, "Sinc-sampled fibre Bragg gratings for identical multiple wavelength operation," *IEEE Photon. Technol. Lett.* **10**(6), 842–844 (1998).
17. C. Fukai, K. Nakajima, J. Zhou, K. Tajima, K. Kurokawa, and I. Sankawa, "Effective Raman gain characteristics in germanium- and fluorine-doped optical fibers," *Opt. Lett.* **29**(6), 545–547 (2004).
18. R. Stolen, "Polarization effects in fiber Raman and Brillouin lasers," *IEEE J. Quantum Electron.* **15**(10), 1157–1160 (1979).
19. R. Stegeman, L. Jankovic, H. Kim, C. Rivero, G. Stegeman, K. Richardson, P. Delfyett, Y. Guo, A. Schulte, and T. Cardinal, "Tellurite glasses with peak absolute Raman gain coefficients up to 30 times that of fused silica," *Opt. Lett.* **28**(13), 1126–1128 (2003).
20. J. Shi, X. Feng, P. Horak, K. K. Chen, P. S. Teh, S.-U. Alam, W. H. Loh, D. J. R. Richardson, and M. Ibsen, "1.06 μm picosecond pulsed, normal dispersion pumping for generating efficient broadband infrared supercontinuum in meter-length single-mode tellurite holey fiber with high Raman gain coefficient," *J. Lightwave Technol.* **29**(22), 3461–3469 (2011).
21. R. Suo, J. Lousteau, H. Li, X. Jiang, K. Zhou, L. Zhang, W. N. MacPherson, H. T. Bookey, J. S. Barton, A. K. Kar, A. Jha, and I. Bennion, "Fiber Bragg gratings inscribed using 800nm femtosecond laser and a phase mask in single- and multi-core mid-IR glass fibers," *Opt. Express* **17**(9), 7540–7548 (2009).
22. A. Mori, H. Masuda, K. Shikano, and M. Shimizu, "Ultra-wide-band Tellurite-based fiber Raman amplifier," *J. Lightwave Technol.* **21**(5), 1300–1306 (2003).

1. Introduction

There has been much interest in rare-earth doped distributed feedback (DFB) fibre lasers in recent years because of a number of very attractive optical performance related parameters [1–3]. In particular they offer a number of advantages over their semiconductor counterparts, including very low noise characteristics and high efficiency because of the much longer interaction lengths between pump and signal. The oscillating wavelength is accurately defined by a Bragg grating written directly into the fibre, and inserting a π phase-shift at, or close to, the centre of the Bragg grating structure helps to ensure both very low lasing threshold and single-frequency operation. These attractive characteristics have led to DFB fibre lasers finding an increasing number of applications spanning from telecommunications requiring low-noise source performance, over range-finding and LIDAR, to acoustic sensing. Rare-earth doped DFB fibre lasers are indeed already commercialised and servicing a number of these markets. In addition to the proven performances of rare-earth doped DFB fibre lasers, a Raman gain based DFB fibre laser would have a number of potential further advantages. These include for example the possibility of generating narrow linewidth low-noise oscillation in wavelength bands outside of what is possible with rare-earth doped materials. Additionally, Raman based fibre laser systems do not suffer from the so-called bottleneck issues sometimes associated with high-concentration rare-earth doped fibres such as for example the Er/Yb co-doped systems, which can limit the efficiency due to thermal effects. Because of that, factors sometimes limiting the possibility of obtaining, and maintaining, stable high-power operation in rare-earth doped fibre laser systems could potentially be evaded by using Raman gain instead.

Raman fibre lasers were demonstrated as early as the 1970s [4]. Very different from their rare-earth doped counterparts, the operating wavelength of Raman fibre laser is only related to the pump wavelength and the Raman shift of the material used. They can therefore in principle be designed to oscillate at any desired wavelength ranging from the visible to the infrared region, pending only the availability of a suitable pump source [5–8]. This makes them very interesting for applications in telecommunications for example, where operation in extended wavelength bands currently is being considered and investigated to meet future capacity demands. However, the typical cavity lengths required for a conventional lumped

silica Raman fibre laser is quite long (tens to hundreds of meters) because of the low Raman gain coefficient (g_r) of germanosilica fibre [4]. Long linear cavity length limits the possibility of generating stable single mode operation from these devices because of the very tight longitudinal mode spacing in multimeter linear cavity systems. However, short cavity Raman fibre laser designs have been proposed by Perlin and Winful [9]. They predicted theoretically that single wavelength operation should be possible from $<1\text{m}$ cavity lengths by writing a fibre Bragg grating DFB structure directly into germanium doped silica fibre [9,10], and pumping it at the corresponding Raman shift wavelength. Further numerical simulations have revealed that a practical R-DFB fibre laser could be made sufficiently efficient from a π phase-shifted grating of only tens of centimetres in length, and ideally it should even exhibit only watt-level threshold [11,12]. Recently, R-DFB fibre lasers at $1.58\text{ }\mu\text{m}$ in a Raman fibre and a highly nonlinear fibre were experimentally demonstrated [13,14], in which the DFB cavity were 12.4cm s long with a π phase shift located at 8% offset from the centre. In that particular work, the threshold powers required for lasing were 39W and 4.3W, respectively. The maximum output they reported was 350mW with the incident pump power of 34W. Instead, we have demonstrated low threshold ($\sim 1\text{W}$) and high power (with up to 2W) R-DFB fibre lasers at $\sim 1.1\text{ }\mu\text{m}$ [15].

In this work we experimentally demonstrate 30cm long Raman DFB fibre lasers with up to 1.6W of output power. The demonstrated lasers operate in a single frequency at $\sim 1.1\text{ }\mu\text{m}$, and have threshold powers in the low Watt regime. We demonstrate lasers in both standard-NA (0.12) and high-NA (0.35) germanosilica fibres, with slope efficiencies of $\sim 74\%$ and $\sim 93\%$ respectively. Numerical results confirm the performance of the lasers, and additionally show, as an example, that even shorter Raman DFB fibre laser devices will be possible by writing phase-shifted Bragg gratings into tellurite fibres which possesses much higher intrinsic Raman gain characteristics than silica.

2. Experimental setup

The schematic diagram of the experimental setup used to generate and analyse the Raman DFB fibre laser oscillation is shown in Fig. 1(a). An unpolarised CW, 1068nm, Yb-doped all-fibre MOPA with a maximum output power of 15W is used as the Raman pump source. The output of this source is spliced to a 1064nm/1117nm wavelength division multiplexer (WDM1) which in turn is spliced to the phase-shifted DFB grating. This layout allow for the backward output power and performance of the Raman DFB laser to be analysed as well. The forward output of the DFB grating is spliced to two cascaded 1064nm/1117nm WDMs (WDM2 and WDM3) to better isolate the forward DFB fibre signal from any residual pump power. The total output power of the Raman DFB fibre laser is measured through the 90% arm of coupler1 and coupler2, both of which are 90/10 couplers at 1117nm. The 10% port is used to monitor the DFB output spectrum with an optical spectrum analyzer (OSA). Herein, the spectra with high resolution bandwidth (RBW) of 0.01nm were measured by using a low power tolerance OSA (Advantest Q8384) and the spectra with low RBW of 0.1nm were measured by using a high power tolerance OSA (Agilent 18640B). All fibre ends are angle cleaved to prevent end-feedback which could perturb the DFB laser. All components (WDMs, couplers and DFB gratings) are mounted on actively controlled heat sinks to control the temperature and better remove any generated heat.

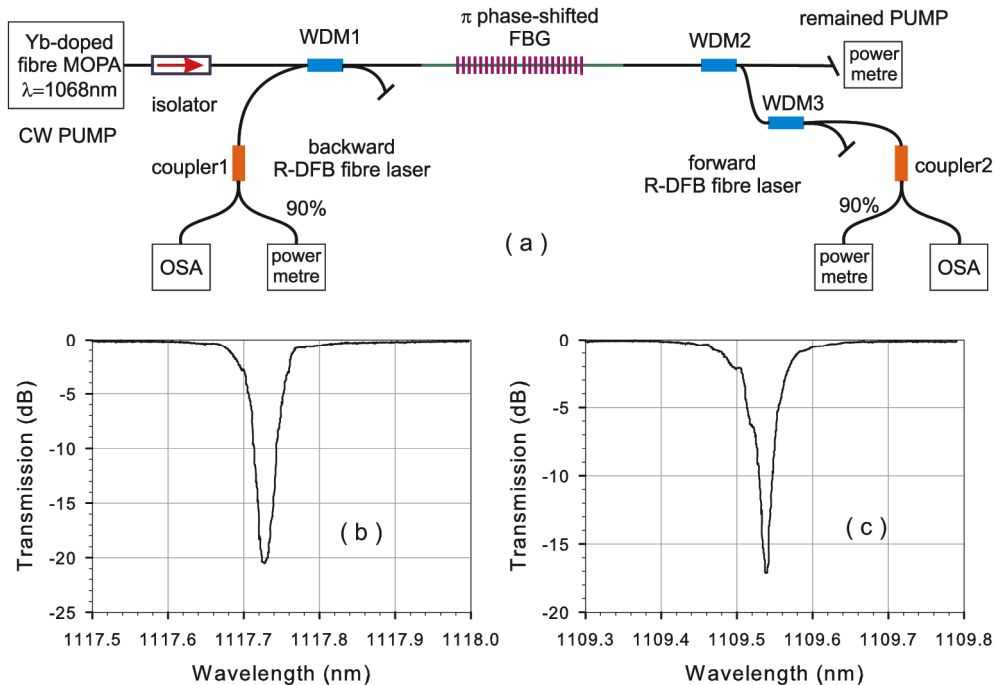


Fig. 1. (a) Schematic diagram of the experimental setup. Passive cold cavity transmission spectra of the DFB gratings in PS980 (b) and UHNA4 (c), measured with a RBW of 0.01nm.

To help demonstrate practical Raman DFB fibre laser operation, we choose two types of commercially available germanosilica (Ge/Si) fibres being the PS980 fibre from Fibercore Ltd. and the UHNA4 fibre from Nufern. Since our system is designed for operation with a high-power Yb-doped fibre pump source at 1068nm, the two fibres are chosen such that they are nearly single-moded in the region of the projected Raman oscillation. The main specifications of the two fibres are: Numerical Aperture (NA) = 0.12-0.14, mode field diameter (MFD) = $6.2 \pm 0.3\mu\text{m}$ (@ 1100nm) and cut-off wavelength = 900nm for PS980, while for UHNA4 the corresponding parameters are NA = 0.35, MFD = $2.6 \pm 0.3\mu\text{m}$ (@ 1100nm) and cut-off wavelength = 1100 nm. The splice loss between the WDMs and the low-NA PS980 is negligible, whilst it is ~0.64dB for the high-NA UHNA4 fibre due to a slight MFD mismatch between the two fibre types. It is worth noting that the PS980 fibre is a boron co-doped Ge/Si fibre whilst the UHNA4 is Ge/Si only. The addition of boron aids the photosensitivity and also increases the Raman gain coefficient marginally compared to a germanium only co-doped fibre of similar NA. The DFB gratings are 30cm long with centre π phase-shifts to help facilitate the lowest possible lasing threshold. They are written directly into the fibres without the aid of hydrogen loading with 244nm CW UV-light using the continuous grating writing technique [16]. The passive cold cavity phase-shifted grating transmission spectra in the two fibres are shown in Figs. 1(b) and 1(c). From uniform test gratings written prior to the phase-shifted DFB gratings the coupling coefficient, κ , of the gratings is estimated to be 37m^{-1} and 30m^{-1} in the PS980 and UHNA4 fibres, respectively. Due to the low refractive index modulation in the gratings ($\sim 10^{-5}$) and absence of photosensitising loading gas, the UV-induced loss in the two fibres is minimal. The total propagation loss is therefore not much higher than the linear loss of the pristine fibres, which is ~20dB/km for PS980 and ~5dB/km for UHNA4 at the projected Raman DFB operating wavelengths. At 1068nm, the unpolarised peak Raman gain coefficients of the two fibres are estimated to be $\sim 0.86 \times 10^{-13}\text{m/W}$ for PS980, and $\sim 1.55 \times 10^{-13}\text{m/W}$ for the UHNA4 fibre, respectively [17]. Table 1 summarizes the key fibre and Bragg grating parameters used for the Raman DFB lasers.

Table 1. Key Parameters of the Fibres and Bragg gratings Used for the Raman DFB Fibre Lasers

R-DFB	Fibre	NA	A_{eff} @ 1100nm (μm^2)	g_r @ 1.06 μm ($\times 10^{-13}\text{m/W}$)	λ_B (nm)	κ (m^{-1})	$L_{\text{DFB gratings}}$ (cm)	L_{total} (incl. pigtails) (cm)
1	PS980	0.12-0.14	30.3 ± 2.9	0.86	1117.73	37	30	38
2	UHNA4	0.35	5.4 ± 1.2	1.55	1109.54	30	30	57

3. Results and discussion

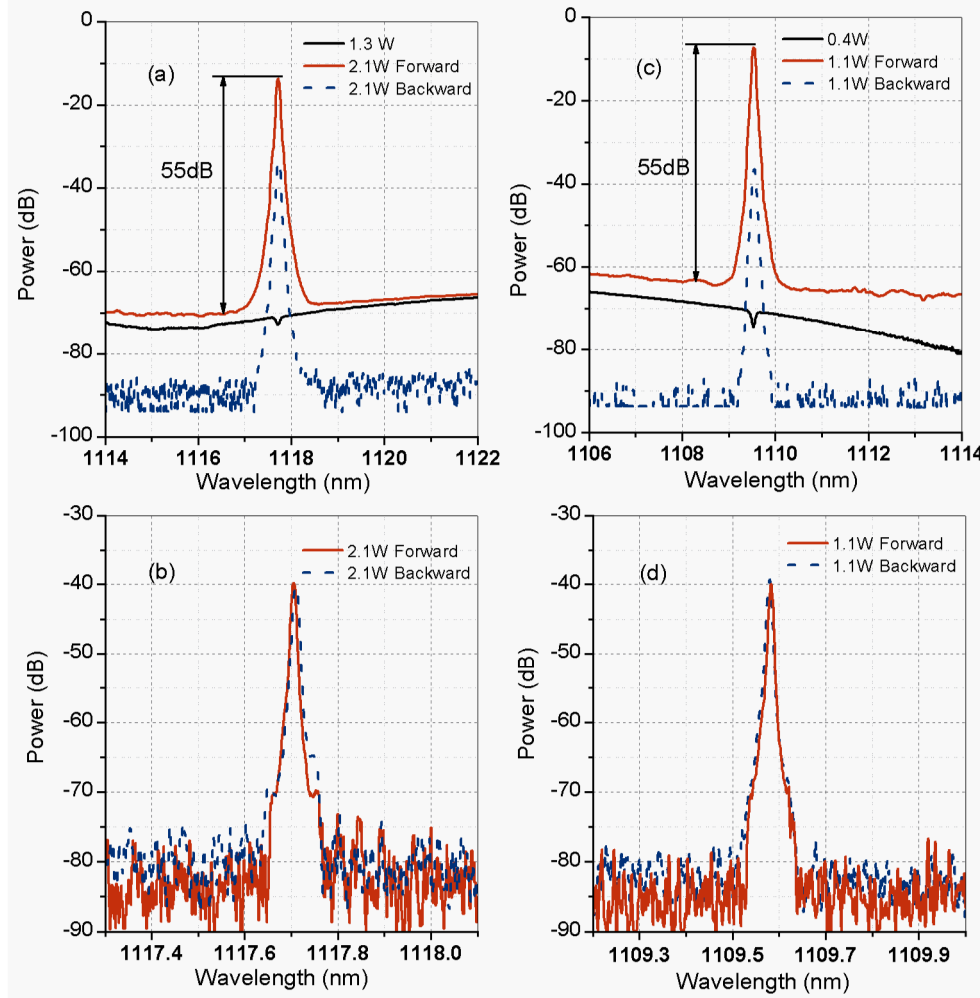


Fig. 2. DFB output spectra just below and just above threshold of R-DFB1 with 0.1nm RBW (a) and 0.01nm RBW (b), and R-DFB2 with 0.1nm RBW (c) and 0.01nm RBW (d). The powers shown in the figure are the incident pump power.

Figures 2(a) and 2(c) show the forward and backward DFB output spectra just below and just above the lasing threshold for the two fibres. The threshold power for lasing is $\sim 2\text{W}$ and $\sim 1\text{W}$ for R-DFB1 (standard-NA fibre) (Fig. 2(a)) and R-DFB2 (high-NA fibre) (Fig. 2(c)), respectively. As is clearly evident the lasing occurs exactly at the Bragg wavelength of the phase shifted grating as expected from a π phase-shifted grating structure. Unsurprisingly, the threshold for lasing is lower in the high-NA fibre since this fibre has the higher Raman gain coefficient due to larger concentration of germanium [17]. Both lasers exhibit more than 50dB

signal-to-noise ratio (SNR) with 0.1nm RBW soon after lasing has started. Figures 2(b) and 2(d) show the DFB output spectra of R-DFB1 and R-DFB2 with a high resolution of 0.01nm in 0.8nm wavelength span. It can be seen clearly that their 3dB linewidths must be less than 0.01nm limited only by the resolution of OSA. More accurate linewidth measurements can be carried out by using for example delayed self-heterodyne or self-homodyne methods [13,14].

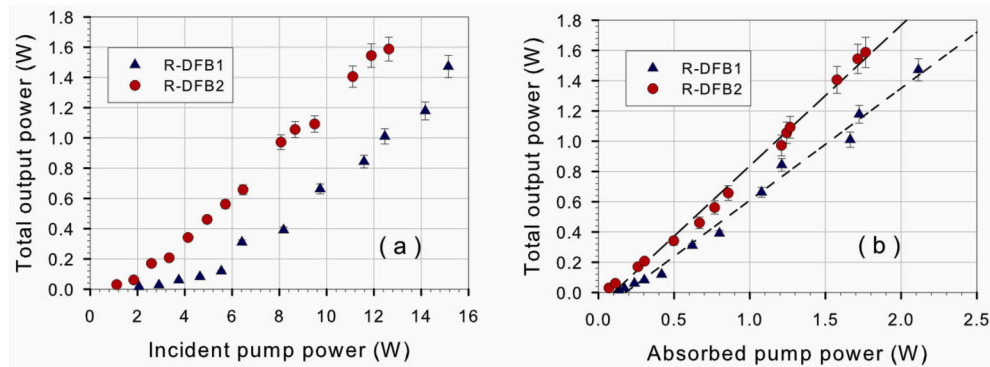


Fig. 3. Total R-DFB output power against incident pump power (a) and absorbed pump power (b).

Figure 3(a) illustrates the relationship between the total R-DFB output power and the incident (launched) pump power for each of the two fibres. The R-DFB output powers are seen to grow slowly for low input powers but gradually increase as the pump power is increased. Although not a particularly good measure of the efficiency due to the non-linear nature of the output power growth with pump power, the output powers are seen to increase with slope efficiencies above 13% in both lasers for pump powers of ~ 3 W above threshold. This efficiency is slightly lower than predicted by simulations, but it could in part be explained by the presence of minor phase and amplitude errors in the gratings [12]. Viewing the slope efficiency of the output power against absorbed pump power gives a better picture of the efficiencies. The measurement of the converted pump power is done by comparing the incident pump power with the remaining pump-power at the output of the DFB gratings, corrected for the insertion loss of WDM2 and the splice point, as shown in Fig. 1(a). In the case of the low-NA R-DFB (R-DFB1) the slope efficiency is found to be $\sim 74\%$, and in the case of the high-NA R-DFB (R-DFB2) it is $\sim 93\%$ as shown in Fig. 3(b). The reason for the lower slope-efficiency from R-DFB1 might be due to the slightly higher propagation loss in this fibre. However, the 93% in R-DFB2 is close to the theoretical quantum conversion efficiency, which is in good agreement with numerical simulations. The maximum output power obtained is ~ 1.5 W for R-DFB1 and ~ 1.6 W for R-DFB2, which to the best of our knowledge is the highest ever reported out power for a DFB fibre laser. The uncertainty in the measured output power is about $\pm 5\%$, due to the use of a thermal power metre and the power variation of the pump source.

Figures 4(a) and 4(c) show the forward and backward output spectra with 0.1nm RBW at the maximum output power. Additionally, Figs. 4(b) and 4(d) display the backward DFB output with 0.01nm RBW of R-DFB1 and R-DFB2 at this power level, respectively. The spectra demonstrate that the high SNR and narrow-bandwidth properties are maintained even at this power level. A slight bandwidth broadening is observed when comparing the forward output spectra with those of the backward spectra, and in the case of the high-NA fibre the SNR is also observed to be slightly reduced although it still remains above 50dB. The reason for the slight broadening and reduction of SNR we believe to be due to co-propagating non-linear interplay between the forward signal and the residual pump power [8]. We hope to report further and give more detailed analysis on these observations in future publications.

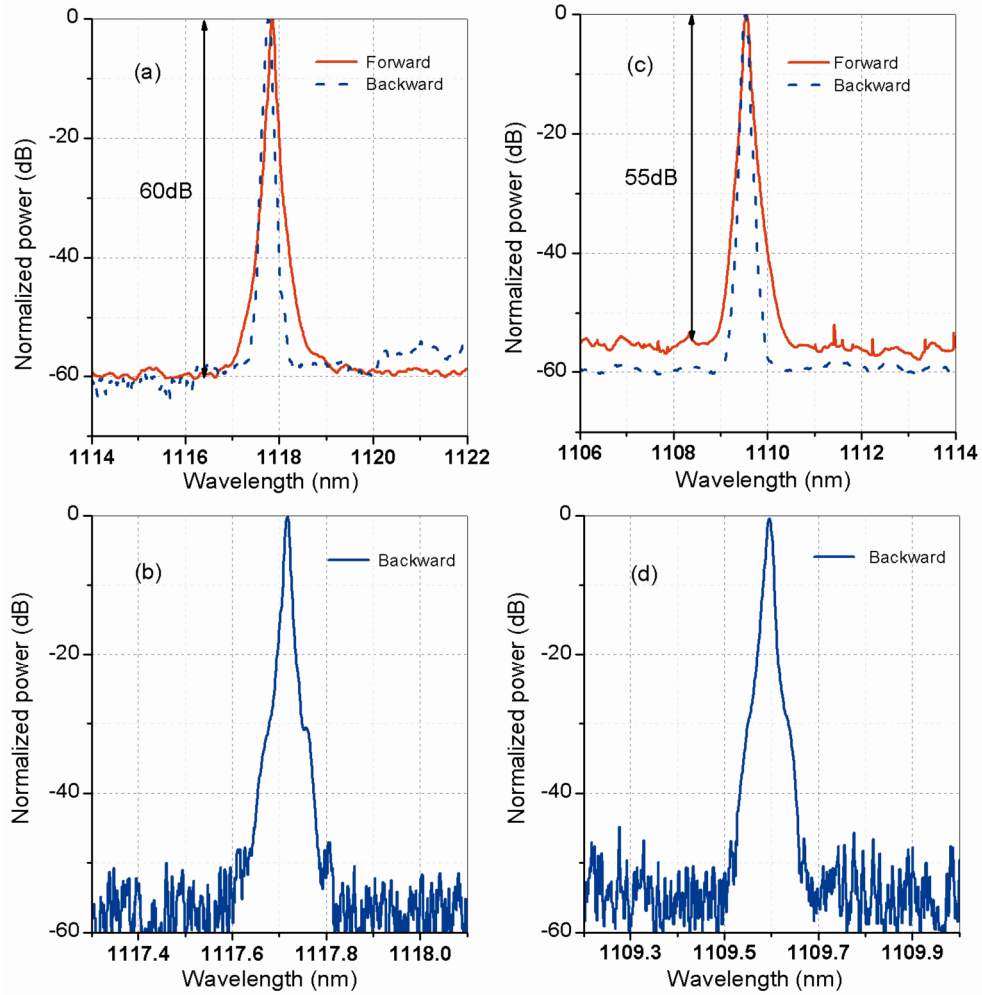


Fig. 4. DFB output spectra at maximum output power of R-DFB1 with 0.1nm RBW (a) and 0.01nm RBW (b), and R-DFB2 with 0.1nm RBW (c) and 0.01nm RBW (d).

4. Theoretical analysis

To further understand the conditions required to achieve oscillation of the R-DFB fibre lasers, we theoretically evaluate the expected threshold powers for a set of different fibre parameters. Our numerical model is based on solving the standard nonlinear coupled mode equations with an implicit fourth-order Runge-Kutta method [11,12]. Previous theoretical results [9,11,12] have shown that the threshold power of the R-DFB lasers is inversely proportional to the peak Raman gain coefficient, g_r , and the length of the DFB grating for constant grating strength, κL . It scales inversely with the square of κL , and linearly with the effective area, A_{eff} , of the fibre. However, an important parameter in any laser is the linear propagation loss, α , of the cavity as well. The effects of this loss were largely ignored in previous reported theoretical works on Raman DFB fibre lasers. It is self-evident that lasing only occurs when the total gain in the cavity exceeds the total loss of the cavity. This loss includes the intrinsic propagation loss of the host fibre together with any losses introduced by components utilised in the laser system. Even though the cavity length is very short for a Raman DFB fibre laser, the signal propagation length is significantly longer because of the multiple cavity roundtrips required for the laser to reach threshold and start oscillating. The influence of α is therefore an

important parameter that cannot be neglected. In the case of a Raman DFB fibre laser, α is composed of the intrinsic fibre loss, the cavity reflection loss determined by κL , together with losses potentially imposed by the inscription process of the grating itself. These losses include for example hydrogen or deuterium loading treatments to enhance the level of photosensitivity, and the choice of laser source used to inscribe the grating and create the refractive index changes [13].

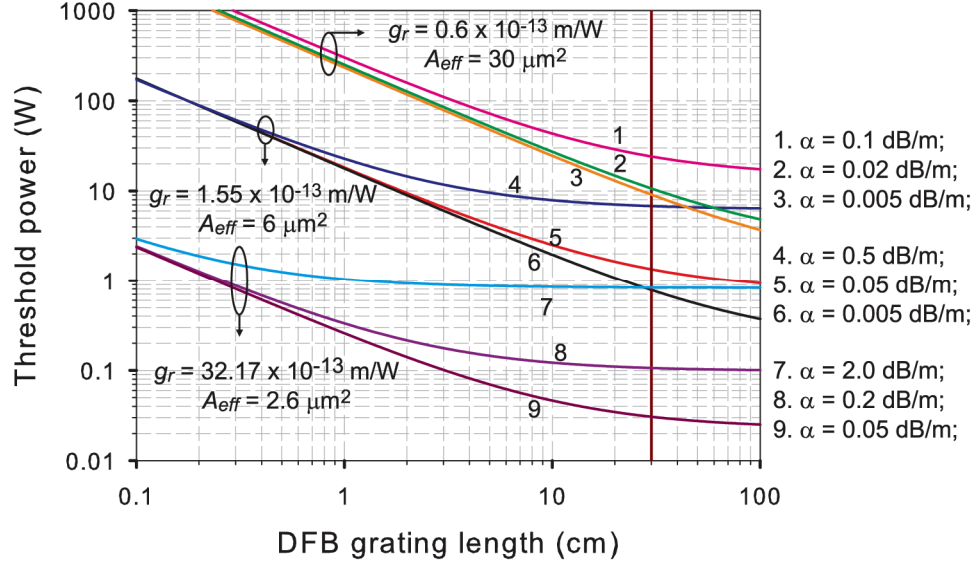


Fig. 5. Simulated incident threshold power against length of centre π phase-shifted Raman DFB fibre lasers for three different fibres. Vertical line indicates the DFB grating length of 30cm.

Figure 5 shows the simulated incident threshold power as a function of the length of a centre π phase-shifted DFB grating for three types of optical fibre that conceivably could be used as the host for R-DFB lasers. In the model the propagation losses of pump and Stokes waves are for simplicity assumed identical. The grating strength, κL , is kept constant at 9 in all the simulated cases considered here. This value is chosen because it both ensures a relatively low threshold power whilst keeping the slope efficiency relatively high [12]. The total cavity loss is varied across a range of values, typical to what could be expected in each of the chosen fibres depending on which grating inscription process is used to form the DFB gratings. As the results indicate, for low levels of loss the reduction of the threshold power follows the expected inverse relationship with increasing length. Unsurprisingly, the results also indicate that the loss ultimately sets the limit to how low the threshold can be irrespective of how long the grating becomes. There is a clear trend in that it is seen to almost always be favourable to increase the length when possible.

Evidently the Raman gain coefficient plays a dominant role in reducing the threshold for these lasers. For standard single mode silica fibre, referring to HI-1060 in this specific case because of the wavelength region employed in this particular work, with an unpolarised peak Raman gain coefficient of $g_r = 0.6 \times 10^{-13}$ m/W and effective area of $A_{\text{eff}} = 30 \mu\text{m}^2$, more than 10W of incident pump power is required to reach threshold when the loss is larger than 0.02dB/m for DFB grating lengths less than 30cm, as indicated by the vertical line intersecting with line 2 in Fig. 5. We choose this particular length here only as an example since it is the length of the R-DFB lasers demonstrated in this work. The lowest possible threshold power in this case is ~9W when only the intrinsic fibre loss is considered (line 3). As the figure also indicates this threshold could be reduced to ~4W for a 1m long DFB grating. By considering a fibre of slightly higher Raman gain, such as for example UHNA4 used in this work, the threshold is reduced by almost an order of magnitude to ~1W for a

30cm long device as long as the losses in the grating are kept below $\sim 0.05\text{dB/m}$ as indicated by lines 5 and 6 of Fig. 5. UHNA4 has a nominal unpolarised peak gain coefficient of $g_r = 1.55 \times 10^{-13} \text{ m/W}$ and an effective area of $A_{\text{eff}} = 6 \mu\text{m}^2$. For higher loss values, although still relatively modest considering certain types of grating inscription methods, the threshold approaches that of the HI-1060 fibre. It is interesting to observe that in the case of 0.5dB/m loss (line 4) the threshold reaches a plateau of $\sim 7\text{--}8\text{W}$ from $\sim 10\text{cm}$ grating length, a level that in this case cannot be reduced further by increasing the length. In reality, increasing the length whilst keeping κL constant will almost always be beneficial in terms of reducing the threshold power, since the value of κ will decrease accordingly. A reduction in the value of κ would typically imply a reduction in the grating inscription induced loss and thus a reduction in the overall cavity loss. The experimental results achieved with this fibre for a 30cm long device indicate that the cavity losses indeed are close to the 0.005dB/m level and thus that the process used for the grating inscription in this work introduce only minimal additional loss. As indicated by line 6 in the figure, the theoretical minimum threshold for a 30cm long DFB grating in this case is $\sim 800\text{mW}$. Note that all these thresholds powers are achieved considering unpolarised Raman gain. If polarised Raman gain is considered the level would scale accordingly as referred to above [18].

Due to the emergence of a variety of low-loss non-silica based fibres with higher values of both nonlinearity and Raman gain coefficient, we also simulate what the likely performance of R-DFB lasers would be in these types of fibres. Tellurite fibres, for example, have recently shown promising potential for efficient Raman amplification [19,20]. Combined with higher values of Raman gain, interestingly, these fibres also exhibit a level of photosensitivity that would facilitate the formation of sufficient strength gratings for R-DFB fibre lasers [21]. Propagation losses in these fibres tend to be slightly higher than those in silica based fibres, so for the simulated examples considered here, we choose values to represent what currently is achievable (Fig. 5, lines 7-9). The unpolarised peak Raman gain coefficient used in the simulations of $g_r = 32.17 \times 10^{-13} \text{ m/W}$, is estimated by measuring the spontaneous Raman spectrum from a tellurite glass bulk sample [20]. For consistency the grating design parameters are kept similar to the cases discussed above. In order to simulate a fibre which also would be transverse single-mode at the operating wavelength considered here an effective area of $A_{\text{eff}} = 2.6 \mu\text{m}^2$ is used in the simulation. As the results show, even with a relatively high loss value of 2dB/m (line 7) $\sim 1\text{W}$ threshold power can be achieved using only a 2cm long DFB grating. Similar to the case of the higher loss in the UHNA4 example given above, the threshold is seen to reach a plateau of $\sim 900\text{mW}$ for increasing grating length rendering a longer length futile. Since current losses in tellurite fibres in reality are somewhat lower at the $\sim 0.05\text{dB/m}$ level [22], in part depending on the purity of the materials used and the fibre design (solid vs. air-suspended core designs), the simulations suggest that threshold levels in the 300mW regime should be possible from only 1cm long devices. As indicated by lines 8 and 9, this level could even be brought to the 100mW level and below, by considering R-DFB gratings of around 10cm in length. Having pump power requirements as low as this would open up for these sources to be pumped using existing pump-diode technology as opposed to higher power pump lasers. Centimetre length lasers in non-silica fibre with DFB level performance such as low intensity and phase noise together with narrow linewidth, would potentially be very attractive for a range of applications in for example point sensing and extended wavelength transmission band telecommunications where transmission beyond $2\mu\text{m}$ currently is being considered.

Similar to rare-earth doped DFB fibre lasers these lasers are tunable via comparable methods because of the available Raman gain bandwidth. The possible operating wavelength regions are more flexible than their rare-earth equivalent since the oscillating wavelength only depends on the availability of a suitable Raman pump wavelength. Cascaded Raman pumping could be used to facilitate the reach of non-standard operating regions starting at pump-wavelength covered by standard fibre or diode technologies for example. This would result in increased flexibility to generate a wide range of different wavelengths with a single fixed pump source.

5. Conclusions

We have experimentally demonstrated highly efficient Raman DFB fibre laser oscillation at $\sim 1.1\mu\text{m}$ from two 30cm phase-shifted Bragg gratings written in two types of passive Ge/Si fibres. The lasers are pumped with up to 15W of CW power at $\sim 1.07\mu\text{m}$ to give narrow linewidth signal output powers in excess of 1.5W in each case. The threshold incident pump power is as low as $\sim 1\text{W}$ in a fibre with an NA of 0.35, and only $\sim 2\text{W}$ for a fibre with a standard NA of $\sim 0.12\text{--}0.14$. Numerical simulations are used to confirm the experimental results. Simulations are furthermore employed to investigate the effects the linear fibre and grating loss on the threshold of the lasers. These confirm that Raman DFB fibre laser oscillation from cm-length lasers with threshold powers in the 100mW regime is possible by considering, for example, passive high-index non-silicate tellurite glass fibre as the host for the lasers. Because of these traits we believe that Raman DFB fibre lasers could play an important role in application areas where narrow linewidth is desirable, and for wavelength operation outside the regions currently only supported by lasers in rare-earth doped fibres. It is worth noting that since Raman DFB lasers can be formed in commercially available standard fibres, the cost of these devices could potentially also be very low.

Acknowledgments

The authors would like to thank useful discussions with Youfang Hu, Neil Broderick, Dejjiao Lin and Xian Feng. Jindan Shi gratefully acknowledges the China Scholarship Council (CSC) for financial support. Shaif-ul Alam acknowledges Engineering and Physical Sciences Research Council (EPSRC) for financial support. Morten Ibsen acknowledges the Royal Society of London for the provisioning of a University Research Fellowship.